J. Ind. Geophys. Union, 29(1) (2025), 26-37

Reservoir characterization using a hybrid of particle swarm optimization: A case study from the Blackfoot field, Canada

Ravi Kant[1*], S.P. Maurya[1], Nitin Verma[1], Raghav Singh[1], K.H. Singh[2], Ajay P. Singh[1], Prabodh K. Kushwaha[1], M.K. Srivastava[1], G. Hema[1], Harsha Raghuvanshi[1] and Richa[1]

[1]Department of Geophysics, Institute of Science, Banaras Hindu University, Varanasi-221005, India

[2]Department of Earth Sciences, Indian Institute of Technology, Bombay, Mumbai-400076, India

[*]Corresponding author: ravigeo@bhu.ac.in

ABSTRACT

The development, management, and optimization of a reservoir depend on precise reservoir characterization. There are several methods for doing this, however in the current work, seismic inversion based on the hybrid particle swarm optimization (HPSO) methodology is used. In this method, a local optimization method called quasi-newton method (QNM), combined with a global optimization method called PSO to maximize their benefits and minimize their downsides are used. The global optimization method takes a lot of time to converge whereas, Quasi-Newton method is rapid, but heavily dependent on the initial model. The present study takes these two limitations into account. To characterize the reservoir, the hybrid PSO uses post-stack seismic data to predict acoustic impedance and porosity in the inter-well zone. The effectiveness of this newly devised method is first evaluated using synthetic data, and then it is applied to the real data from the Blackfoot area in Canada. The findings show that for both the synthetic and real data, the inverted outcomes closely match the observed data. The analysis anticipated that the inter-well acoustic impedance and porosity volume would vary from 6000 to 12000 m/s*g/cc and 5-22%, respectively. These volumes display extremely detailed subsurface data. The analysis of inverted findings reveals an abnormal zone inside the two-way transit time frame of 1045 to 1065 ms, ranging from low-impedance 6500-9000m/s*g/cc, and high porosity >15%. This unconventional area is classified as a reservoir. The method is particularly useful in nearby regions where detailed subsurface information needs to be estimated, even with limited prior data.

Keywords: Seismic inversion, Hybrid optimization, Particle swarm optimization, Quasi-newton method, Reservoir characterization, Blackfoot field (Canada)

INTRODUCTION

Reservoir characterization is a multidisciplinary process in the field of geosciences encompassing geology, geophysics and petroleum engineering. It involves the detailed analysis and description of subsurface reservoirs to understand their properties and behaviour. The primary goal of reservoir characterization is to obtain a comprehensive understanding of the reservoir's geological, petrophysical, and fluid properties (Maurya et al., 2020; Kumar et., 2024; Singh et al., 2024). This information is crucial for optimizing oil and gas recovery strategies and making informed decisions throughout the life cycle of a reservoir. Reservoir characterization based on seismic inversion is a crucial process, a technique used to extract detailed information about the subsurface properties of a reservoir by analyzing seismic data that includes properties such as rock and fluid types, porosity, permeability and acoustic impedance. Several techniques are available, but seismic inversion is used here to characterize the reservoir. This method has become quite popular and requires less prior information for implementation (Maurya and Singh, 2018; Kant et al., 2024a).

Various techniques for seismic inversion are continually evolving (Russell et al., 2003; Kant et al., 2024b), which are broadly classified into two categories: direct inversion and indirect inversion. In direct inversion methods, the acquired data is directly used to derive subsurface information. Conversely, indirect inversion methods involve creating a subsurface model and generating synthetic data, adjusting the model to minimize the difference between synthetic and recorded data. This indirect approach is advantageous as it is less affected by inaccuracies or noise in the data, leading to more robust results (Maurya and Sarkar, 2016; Hema et al., 2024). To adjust the subsurface model in seismic inversion, various optimization methods are typically employed. Optimization seeks to determine input values for an objective function that maximize or minimize its output, essentially minimizing the discrepancy between the model and the real Earth data. These techniques are categorized into local and global optimization methods. In local optimization, algorithms follow the downward slope of the cost function's topology, using gradient information to adjust the model and converge to the nearest minimum, based on the starting model's position. However, local methods may get trapped in a local minimum unless the initial guess is close to the global minimum, especially when dealing with multimodal cost functions. On the other hand, global optimization algorithms aim to converge to the global minimum, even in the presence of complex, multimodal cost functions. Examples of global optimization methods include the Monte Carlo method, genetic algorithms, particle swarm optimization (PSO), simulated annealing, while local optimization methods include, steepest descent, conjugate-gradient, Newton's method and Quasi-Newton methods.

The primary objective of any optimization technique is to determine the optimal solution to a problem, which often

involves multiple factors. The distinction between local and global optimization reflects the different search strategies employed by these algorithms. The initial choice of the model significantly impacts the effectiveness of optimization methods such as matrix inversion, gradient descent, or the conjugate gradient method (Maurya et al., 2023). For handling erratic multimodal functions, PSO and the quasi-Newton method are effective strategies. Quasi-Newton methods, which extend Newton's approach by using updated approximations of the Hessian matrix, allow for faster convergence without the need to compute the entire Hessian matrix (Shanno, 1970). In seismic inversion, the primary objective is to determine subsurface acoustic impedance and porosity, which are key geophysical parameters that reveal rock and fluid types beneath the Earth's surface.

Seismic reservoir characterization is essential in integrated exploration and reservoir studies, providing a comprehensive understanding of reservoir structures and properties (Bosch et al., 2010; Bonnans et al., 2006; Kushwaha et al., 2023). In modern prospect evaluation, in reservoir characterization and geological modelling, geophysical techniques have become critically important. Identifying deeper reservoirs has historically posed challenges in exploration, with traditional reservoir characterization methods often increasing both costs as well as risks. Integrated seismic inversion and reservoir characterization have emerged as vital tools to address these challenges, offering critical insights that enhance exploration and production processes, particularly in complex and deep reservoirs (Broyden, 1970; Du and Macgregor, 2010). The main objectives of this study are to evaluate the efficiency of hybrid optimization-based seismic inversion, leveraging seismic data, and to identify potentially productive zones within the Blackfoot field of Alberta, Canada (Simin at al., 1996; Dufour et al., 2002). This analysis is especially relevant for offshore projects, where identifying promising zones can be difficult due to the lack of well-log data. The analytical procedures are conducted using MATLAB and the findings are presented through a comparative analysis of the outcomes obtained from the hybrid optimization approach.

HYBRID PARTICLE SWARM OPTIMIZATIONS (HPSO)

A hybrid algorithm combines two or more distinct approaches to address the same problem, commonly implemented in programming languages such as C++ or Matlab. Depending on the data, the algorithm may dynamically choose between these approaches. This integration is typically performed to amalgamate desirable features from each approach, resulting in an algorithm that surpasses the individual strengths of its components (Nocedal and Wright, 1999). Unlike the simple combination of various algorithms targeting different problems, a hybrid algorithm specifically involves blending approaches designed to solve the same problem but with differences, particularly in performance. Many algorithms can be viewed as compositions of smaller components, and hybrid optimization stands out for its success in maximizing the advantages of diverse techniques while minimizing their respective drawbacks, ultimately leading to enhanced results (Maurya and Singh, 2020). In the context of optimization, a hybrid function persists with the optimization process after the initial solver concludes. In this scenario, a hybrid function incorporates elements of both the quasi-newton's method and the particle swarm optimization solver. By refining the relatively coarse solution provided by the first solver, a hybrid function can converge to a more precise and accurate solution. The flow chart of hybrid particle swarm optimization shown in Figure 1.

In this study, we conducted the inversion of post-stack seismic reflection data to derive subsurface acoustic impedance and porosity, utilizing the global optimization technique known as particle swarm optimization along with quasi-newton method. While global optimization is not influenced by the starting model, its drawback lies in the prolonged time it takes to reach the optimal solution, thereby extending the timeline and increasing the costs of exploration projects. On the other hand, the convergent time of local optimization, specifically quasi-newton method, is very less but needs good starting model. If the starting model is distant from the globally optimal solution, the process can become trapped in local minima, yielding unsatisfactory results. The present work aims to address these challenges by proposing a method that combines particle swarm optimization with quasi-newton method. The objective is to allow particle swarm optimization in a specific time frame to obtain results close to the ideal solution. As achieving the exact optimal solution may take an indefinite amount of time, expecting it within the allocated time frame is impractical. Once a reasonable proximity to the ideal solution is reached, local optimization techniques can be applied, using the particle swarm optimization results as a baseline model. This approach reduces the reliance on local optimization on the initial model, facilitating a rapid convergence to the optimal outcome. Given the simplicity and minimal specialized knowledge required for particle swarm optimization and quasi-newton method, they are recommended for global and local optimization, respectively. In this study, the integration of global and local optimization was achieved through the execution of the following steps.

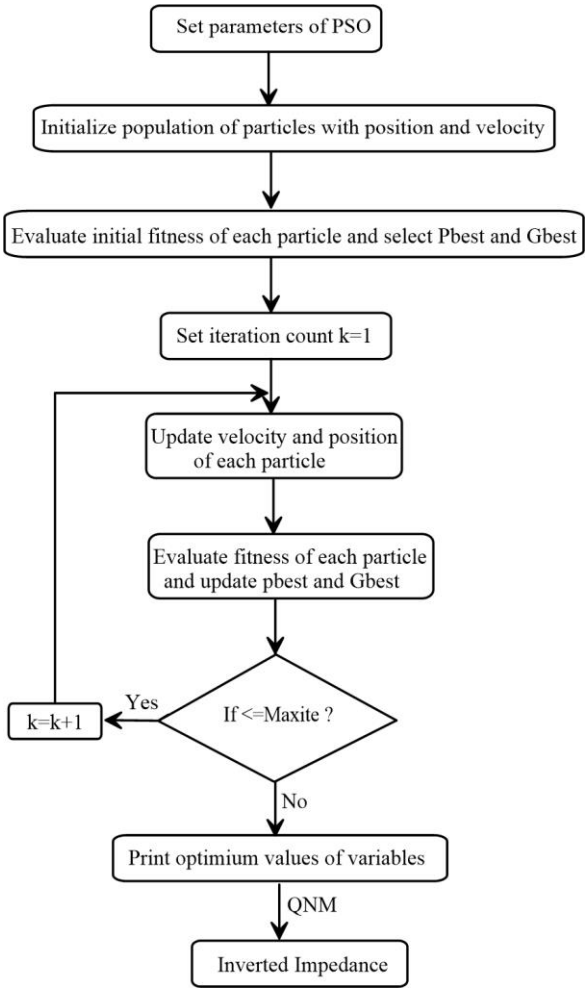

Figure 1. The flowchart representing the workflow of the developed methodology to combine the particle swam optimization and quasi-newton method**.**

1. Select desired seismic and well-log data as input.
2. Transforming depth into time is undertaken to enable the utilization of seismic data in the time domain alongside well-log data in the depth domain.
3. The initial population, comprising acoustic impedances and porosity is generated using a chosen PSO operator implemented for this purpose.
4. Utilizing the given formula, reflectivity is calculated from impedance as follows.

$$R_{modeled(i)} = \frac{Z_{modeled}(i+1) - Z_{modeled}(i)}{\left(Z_{modeled}(i+1) + Z_{modeled}(i)\right)} \quad (1)$$

5. Compute synthetic trace using the formula below.

$$Synthetic\ trace\ (t) = w * r = \int_0^{\infty} r(n)w(n-t)dn \quad (2)$$

where t is time and n is the data index number. When using sampled data, the linear discrete convolution's integral transforms into a sum and can be written as,

$$Synthetic\ trace\ (t) = w * r = \sum_{n=0}^{n=N} r(n)w(n-t) \quad (3)$$

6. Use the formula below to determine the RMS error (fitness function) between the synthetic data and the input seismic data.

$$\text{RMS Error (E)} = \frac{1}{n}\sqrt{\sum_{j=1}^{n}(S_{obs}^{i} - S_{mod}^{i})^2} + \frac{1}{n}\sqrt{\sum_{j=1}^{n}(Z_{obs}^{i} - Z_{mod}^{i})^2} \quad (4)$$

Where n is the total number of sample points, S^i_{obs} is input seismic data at the i^{th} sample, S^i_{mod} is the synthetic trace at the i^{th} sample. The other part of the equation is used here to constraints solution and this information comes from the prior study i.e. well-log in our case. Z^i_{obs} is the impedance at i^{th} sample estimated directly from well log data and Z^i_{mod} is the impedance at i^{th} sample generated by the genetic algorithm in its population.

7. Modify the initial population to reduce RMS error as much as possible within a limited time interval by repeating steps 3 to 6. The output of this step will be acoustic impedance (say, AI_0) that satisfies equation 4.
8. Use a QNM by choosing the initial model (AI_0) as the output of the Particle Swarm Optimization.
9. Compute the Hessian matrix with the value of gradient, model, and objective function.
10. Calculate the RMS error using equation 4.
11. Identify the best solution based on the RMS error and modify the new solution based on the best solution.
12. Check whether the new solution is better than the existing best solution or not.
13. Repeat steps 9 to 12 to terminate the program, and get desired acoustic impedance.

After the mathematical formulation of the hybrid approach, which integrates particle swarm optimization with the quasi-Newton method, the methodology was assessed using synthetic data.

RESULTS AND DISCUSSION

Synthetic example to test algorithm

To test the developed hybrid particle swarm optimization, a synthetic data inversion was conducted. Since the synthetic model has known impedance, it allows for comparison with the inverted impedance, enabling us to monitor the algorithm's effectiveness. The synthetic data is generated using a convolution model, where a seismic wavelet is convolved with the Earth's reflectivity. In convolution modeling, it is assumed that plane waves travel across horizontally homogeneous layers' boundaries, disregarding the impacts of geometric divergence, elastic absorption, wavelet dispersion, transmission losses, mode conversions, and multiple reflections. To retrieve the plane-wave amplitudes of primary P-wave reflections, the seismic data needs to undergo processing to eliminate these effects.

Equations 1, 2, and 3 are employed to generate a synthetic seismogram, utilizing a seventeen-layer model and a Ricker wavelet. The Ricker wavelet is selected due to its effectiveness in representing seismic sources with a zero-phase wavelet, which is commonly used in seismic modeling. The Ricker wavelet employed in this study has a central frequency of 45 Hz, which is chosen to match the dominant frequency typically observed in the target geological formations. The wavelet's amplitude spectrum is characterized by its peak at the central frequency, with symmetrical decay on either side, ensuring that it effectively captures the seismic response of the modeled subsurface layers. The time duration of the wavelet was selected to provide adequate resolution while maintaining the wavelet's compact nature, ensuring minimal side lobes and reducing interference between reflections from different layers. By using this specific Ricker wavelet, we aimed to balance resolution and penetration depth, providing a clear and accurate synthetic seismogram that aligns well with the characteristics of the seventeen-layer model. Input parameters essential for generating synthetic data are presented in Table 1. The equation $AI = denstiy\ (\rho) * velocity(V_p)$ is utilized to calculate acoustic impedance, incorporating the provided values for density and the p-wave velocity model.

Subsequently, the synthetic data underwent the hybrid optimization process. The objective is to employ an algorithm for the conversion of synthetic data into subsurface acoustic impedance. Addtionally, the generating synthetic data generated to cross-verify the inverted impedance with the predicted impedance. The initial two panels of Figure 2 illustrate the velocities and densities of the 17 layers, utilized as input for synthetic data creation. Futhermore, by multiplying the velocity and density values depicted in panels 1 and 2, one can promptly derive an acoustic impedance. This impedance is then further transformed into reflectivity to produce synthetic data, which is convolved with a Ricker wavelet. Figure 2 panels 3, display this synthetic data along with a solid black line.

In Figure 2, panel 4 illustrates the outcome obtained after applying hybrid optimization to convert it into acoustic impedance. Given the expectation that these two impedances should closely resemble each other, the inverted impedance is compared against the original impedance, which is synthetically generated. Moreover, panel 3 of the hybrid optimization presents a synthetic trace produced using the inverted impedance, allowing a comparison with the original synthetic trace. Figure 2 demonstrates a notable alignment between the inverted impedances and the recreated synthetic impedances for hybrid approaches. The correlation between the hybrid optimization and the modeled original trace is recorded at 0.99. The figure indicates a strong fit between both impedances, affirming the effectiveness of the

technique, as evidenced by the 0.99 correlation between the original and inverted impedance from the hybrid. Further, Figure 3 showcases a cross-plot depicting the original and inverted acoustic impedances achieved through hybrid optimization techniques. The close alignment of results is evident in these cross plots, where scatter points closely approximate the best-fit line. A thorough examination of the cross plot highlights the proximity of data points from the hybrid optimization strategy to the best-fit line, underscoring the effectiveness of the Hybrid algorithm. Based on the analysis, it is decided to apply the created hybrid optimization to real data from the Blackfoot Field in Canada.

Table 1. Observed and modeled AI for synthetic data case comparison.

S.No.	Layers	Impedance	Inverted impedance	Change (%)
1	Layer 1	7040	7147.44	1.0744
2	Layer 2	9065	8662.75	4.0225
3	Layer 3	5700	6341.70	6.417
4	Layer 4	7425	7399.50	0.255
5	Layer 5	10040	9999.57	0.4043
6	Layer 6	8225	8099.61	1.2539
7	Layer 7	9500	10184.16	6.8416
8	Layer 8	11700	11500.89	1.9911
9	Layer 9	6300	6533.15	2.3315
10	Layer 10	10455	10597.13	1.4213
11	Layer 11	7425	7423.60	0.014
12	Layer 12	13500	13700.36	2.0036
13	Layer 13	11700	12156.97	4.5697
14	Layer 14	10000	10198.94	1.9894
15	Layer 15	14144	13999.97	1.4403
16	Layer 16	15568	16041.08	4.7308
17	Layer 17	12720	12911.08	1.9108

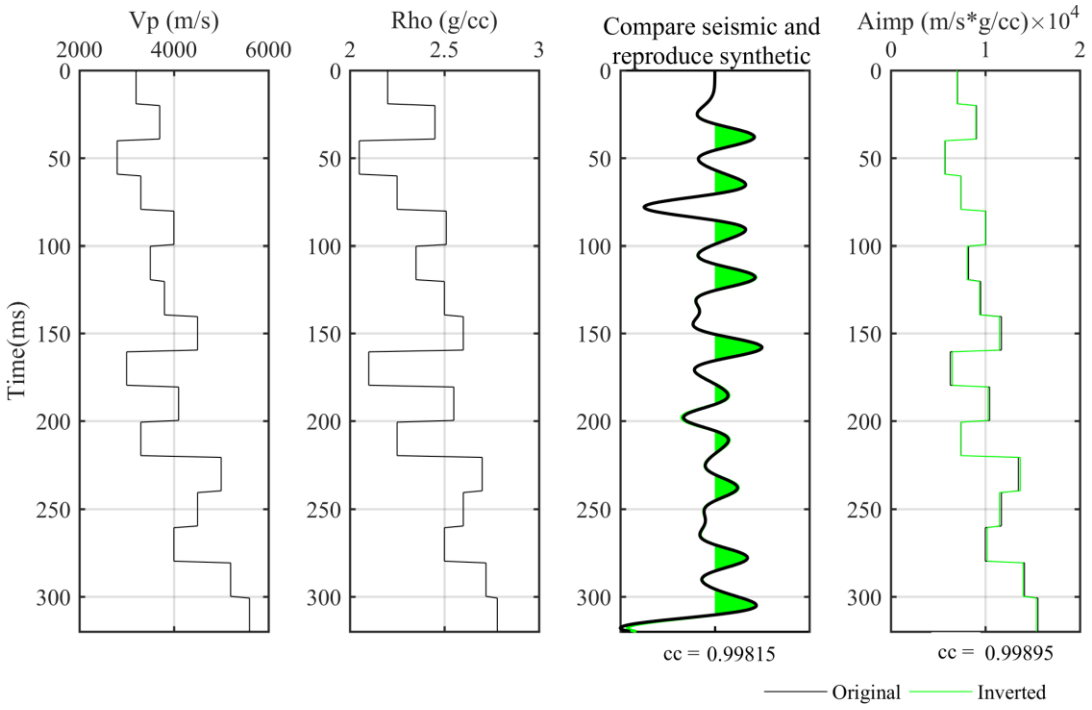

Figure 2. Display of the outcomes of the 1D convolution model applied to synthetic data and seismic inversion.

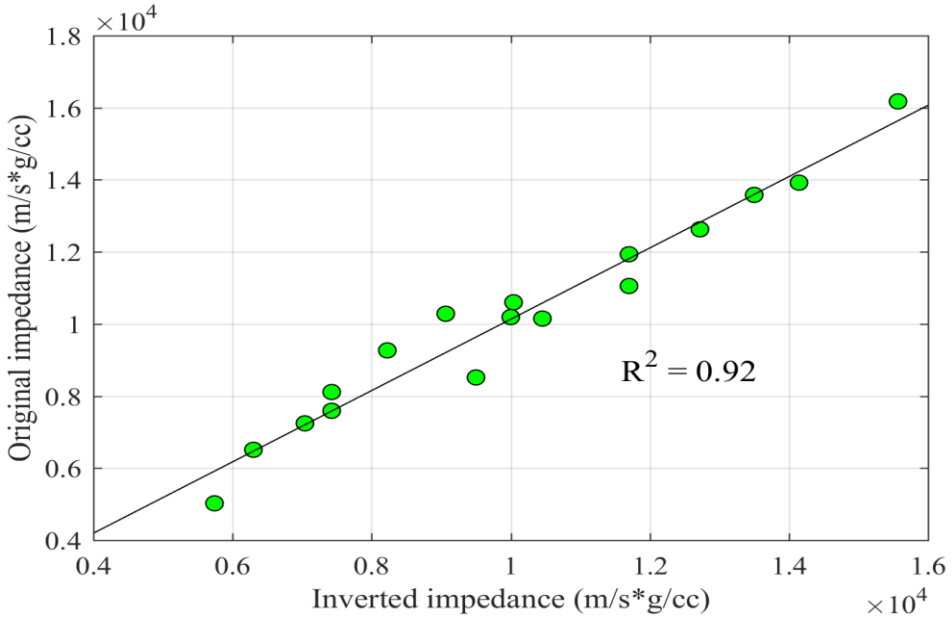

Figure 3. Cross plot between original impedance and inverted impedance

Application to real field data from the Blackfoot field, Canada

The hybrid PSO is applied to data from the Blackfoot Field, Alberta, Canada, in a two-step process. First, a specific seismic trace (composite trace) corresponding to the location of a well or a nearby area is selected, and hybrid optimization is performed on this trace. In the second step, the entire seismic volume is inverted to generate acoustic impedance and porosity volume for the zone between the wells. In this study, well-log data is utilized alongside seismic data to constrain the solution. Since the well-log data is recorded in depth and the seismic data in time, these two datasets cannot be directly integrated. Therefore, a depth-to-time conversion is crucial before performing the inversion. Interpreting horizons within several kilometers of the study area, offers valuable insights into the subsurface structure and helps estimate the depth of geological units. Although the well-log data is manually converted from depth to time (ms), directly aligning it with seismic data is not feasible. Before commencing the inversion process, it is imperative to compute the connection between porosity reflectivity (R_φ) and impedance reflectivity (R_Z), employing the following formula.

$$R_Z = \frac{1}{2}[\log(z_{i+1}) - \log(z_i)] \quad (5)$$

$$R_\emptyset = \frac{1}{2}\left[\left(log\left(\frac{\emptyset_{i+1}}{1-\emptyset_{i+1}}\right)\right) - \log\left(\frac{\emptyset_i}{1-\emptyset_i}\right)\right] \quad (6)$$

In this context, where z_{i+1} and $\emptyset_{i+1}$ represent the impedance and porosity of the $(i+1)^{th}$ layer, and (z_i) and $(\emptyset_i)$ denote the impedance and porosity of the ith layer, respectively. Eqs. 5 and 6 are employed to compute the correlation factor (g), representing the slope of the fitted line. Figure 4a displays a cross plot of porosity reflectivity and acoustic reflectivity, where the best-fit line yields a slope of -0.14. This correlation factor is utilized to generate a porosity wavelet by multiplying the g factor with the impedance wavelet directly extracted from the seismic data. Figure 4b illustrates a comparison between the porosity wavelet and the impedance wavelet, revealing their reverse polarity and the inverse proportionality between porosity and impedance.

Additionally, lower and upper bounds are employed to further confine the search space within the desired range. In this research, the upper and lower bounds were based on the well-log data, and Figure 5 illustrates the results of the inversion analysis for the composite trace near wells 01-08 using HPSO. Figure 5 presents the low frequency impedance and porosity model model (blue solid lines) generated from well log data alongside the lower and upper bounds (dotted blue lines). A comparison of the original (black solid line) and inverted acoustic impedance and porosity (red solid line) is depicted. The AI and porosity derived from well-defined data and inverted data exhibit good agreement. The peak-to-peak values of acoustic impedances and porosity may not match due to the frequency range difference between well log data (20 to 40 kHz) and seismic data (typically 10 to 80 Hz). The correlation between well-log data of impedance and porosity with inverted impedance and porosity obtained through HPSO is 0.79 and 0.71, respectively.

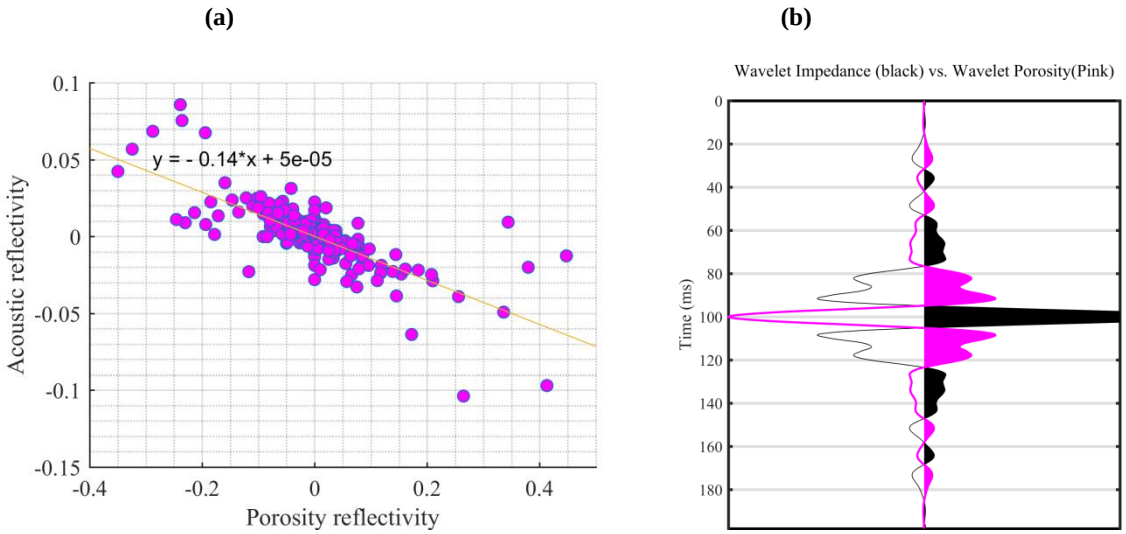

Figure 4. **(a)** A cross plot depicting the relationship between acoustic reflectivity and porosity reflectivity for well 01 − 08_logs, is indicated by a best-fit linear trend, revealing a correlation factor (g = −0.12). **(b)** Comparison between the statistical wavelet (black) and the porosity wavelet (pink), which is generated through the multiplication of the correlation factor with the statistical wavelet.

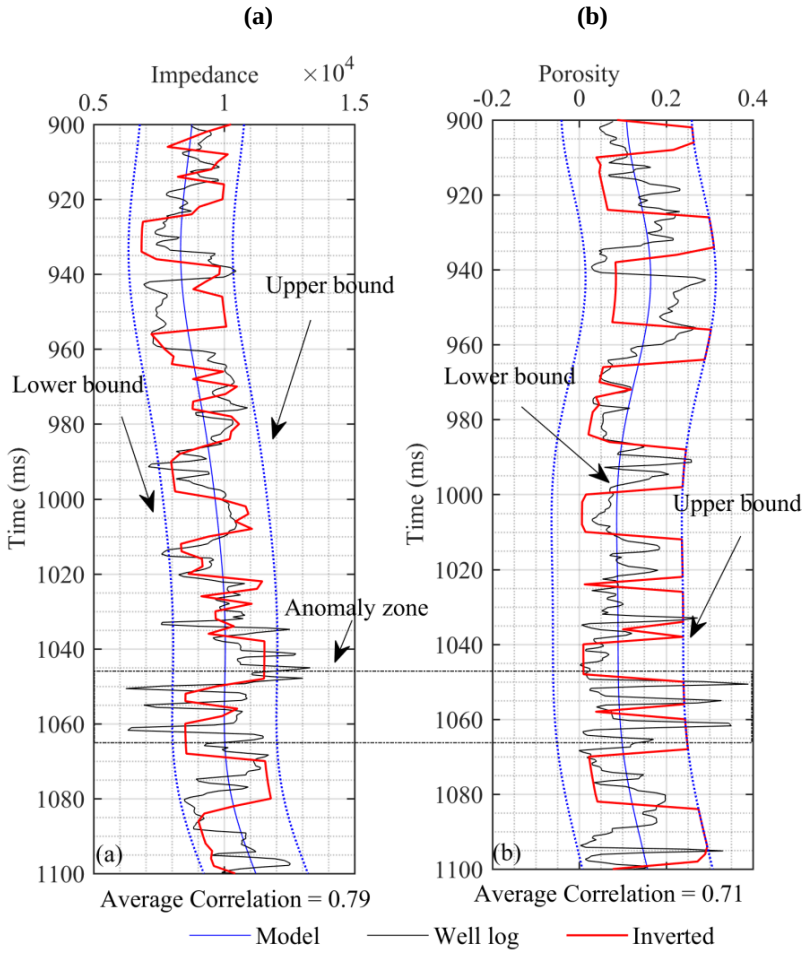

Figure 5. Composite trace analysis near the well 01-08 logs, **(a)** impedance, **(b)** porosity

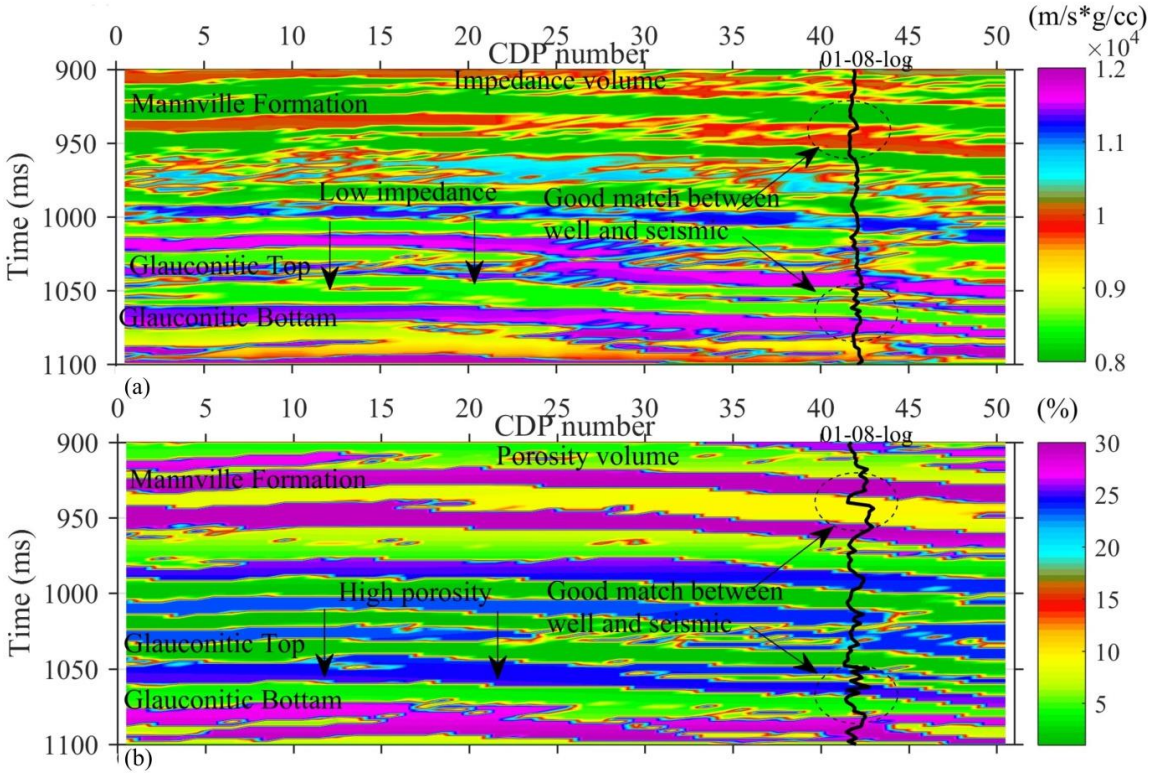

Figure 6. Inverted volume section estimated through HPSO. **(a)** Inverted impedance section and **(b)** porosity volume with well log01-08 log

Following that, the hybrid optimization techniques are applied trace by trace to the CDP stack section to determine the impedance and porosity volume. The inversion is conducted trace by trace, and after inverting all seismic traces using HPSO, the results are plotted against two-way travel time in Figure 6a and 6b, respectively. Figure 6a indicates a good match between the 01-08 log impedance with inverted impedance, with the low impedance zone identified between 1040 and 1065 ms. The boundary at 1040 ms is recognized as a high reflecting layer, as it is surrounded by a high impedance layer (> 11000 m/s ∗ g/cc). Subsequently, Figure 6b presents the porosity volume created by projecting porosity throughout the entire seismic section and the variation of the porosity section at inline 1 with a two-way travel time of 900-1100 milliseconds. The inverted results reveal a very high resolution of the subsurface with layer information, surpassing the interface information provided by the input seismic data. It is observed that the porosity varies from 1 to 30 percent in the study region, and the high porosity zone (> 20%) is situated between 1040 and 1065 ms two-way travel time. The well-log porosity also exhibits a very good agreement with the inverted porosity. Analysis of Figures 6a and 6b reveals that the low impedance zone identified in the inverted impedance section, corresponds to a region of high porosity. This unusual zone, already interpreted in the composite trace between 1040 to 1065 ms two-way travel time, is characterized as a reservoir, specifically a sand channel. In Figure 7, the total variance in inverted impedance and porosity across the 3D volume is illustrated, making it easier to distinguish different zones in this region.

Furthermore, the inverted synthetic traces, generated from the inverted impedance using forward modeling, are compared with the Blackfoot seismic data in Figure 8. Additionally, an inverted synthetic derived from porosity is estimated and similarly compared with the Blackfoot seismic data. The figure is organized into two columns: the first column presents the comparison between the Blackfoot seismic data and the reproduced synthetic traces from both inverted impedance and porosity, while the second column highlights the differences between these comparisons. The replicated synthetic and Blackfoot seismic closely align with each other, as evident in the images. The calculated average correlation between Blackfoot seismic and reproduced synthetically is 0.97 and 0.88, demonstrating a notably high value. These qualitative and quantitative analyses, showcase the effectiveness of the algorithm in this context.

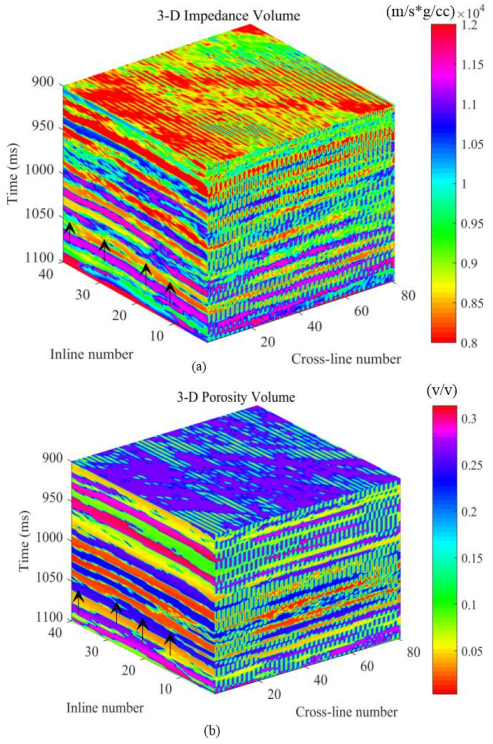

Figure 7. (a) The 3D volume of inverted impedance, and **(b)** porosity, along with the black arrow, highlights the sand channel characterized by low acoustic impedance and high porosity.

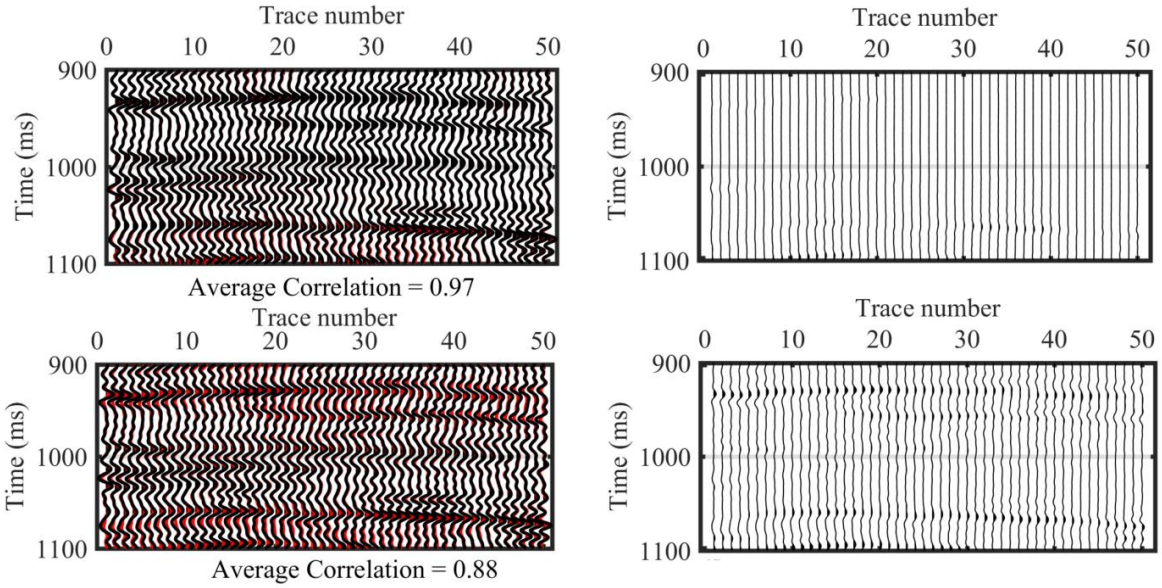

Figure 8. The first columns, Blackfoot seismic and replicated synthetic sections derived from the inverted impedance and porosity estimated through HPSO, respectively. The second column, shows the difference between real and synthetic traces.

Figure 9 illustrates the variance in error with iterations for impedance and porosity. In Figure 9a, the average error for impedance decreases from 2.0 to 1.7 when the stopping criterion is set to 1800, underscoring the effectiveness of particle swarm optimization in yielding improved outcomes. Furthermore, the quasi-Newton method has undergone 1700 iterations, significantly reducing the iteration error. In the case of porosity, Figure 9b demonstrates the error minimization from 2 to 0.55 achieved by HPSO, spanning up to iteration 3100.

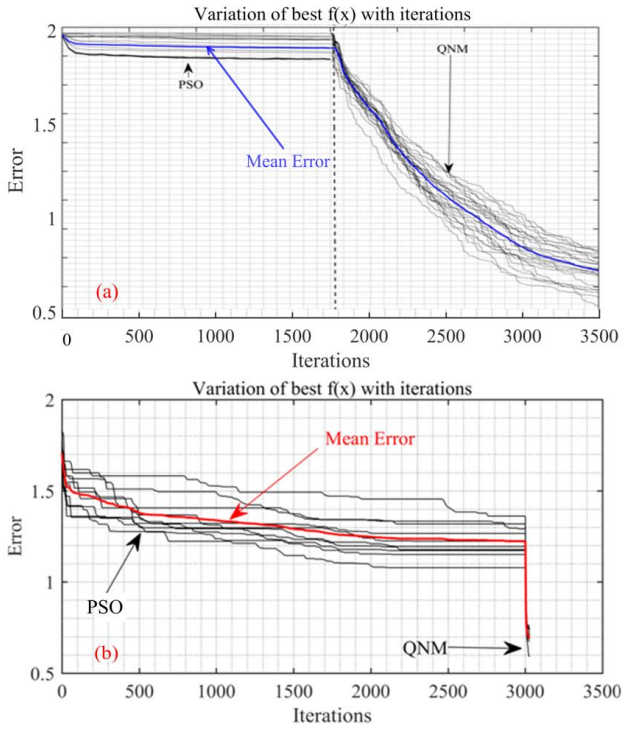

Figure 9. The error variation with iteration is depicted **(a)** for impedance inversion and **(b**) for porosity inversion.

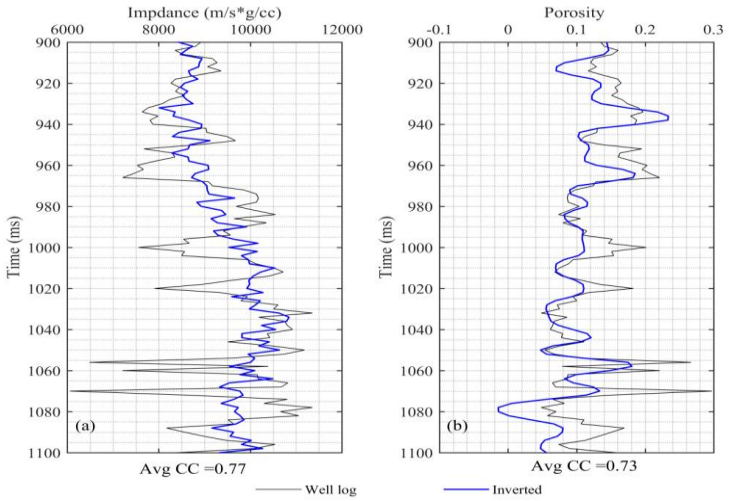

Figure 10. Composite trace analysis near the well 01-08 logs, **(a)** impedance, **(b)** porosity.

Standard inversion results

To compare our results, we selected model-based inversion (MBI), a standard seismic inversion technique widely recognized for its accuracy and reliability in estimating subsurface properties. By comparing our outcomes with those from MBI, we can effectively evaluate the accuracy of our hybrid optimization approach. MBI is a form of local optimization that relies on the least squares method, and its effectiveness is highly dependent on the accuracy of the initial model. If the initial model is inaccurate, the optimization process may become trapped in a local minimum of the misfit function, hindering the accurate extraction of the true subsurface earth model, including impedance and porosity. We first applied MBI techniques at the well location, where the inverted results for impedance and porosity, closely matched the well's actual impedance and porosity, as shown in Figure 10

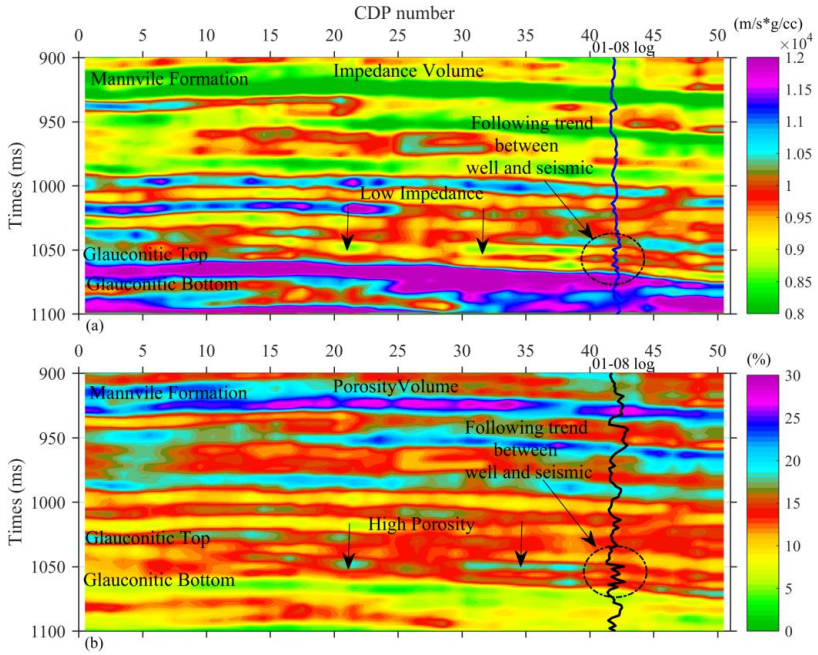

Figure 11. The application of model based inversion and its use for prediction of **(a)** impedance and **(b)** porosity volume

Following these successful results at the well location, we extended MBI to the full volume of seismic data to extract impedance and porosity, as illustrated in Figure 11. Figure 11a shows the inverted impedance, demonstrating that the anomaly zone aligns well with the well data, while Figure 11b presents the porosity volume, revealing the anomaly in patches. However, compared to the hybrid method, these results more effectively resolve thin layers within the anomaly zone, producing high-resolution impedance and porosity volumes. In conclusion, while MBI struggles to resolve thin layers and produces results in a patchy form, the hybrid PSO method effectively resolves both impedance and porosity zones, offering more detailed information about the reservoir zone.

CONCLUSIONS

In the present study, a seismic inversion based on hybrid optimization techniques namely particle swarm optimization (PSO) along with quasi-newton methods (QNM) is applied. The PSO is a global optimization technique which takes large time to converge, whereas QNM is local optimization technique and largely depends on the initial model. The present study combines these two methods together in order to reduce their drawback and enhance their benefits in order to characterize reservoir. These optimization methods require advanced computing capabilities and expertise, they prove to be powerful tools for obtaining high-resolution subsurface information. The inclusion of prior information (well log) in these inversion methods has been demonstrated to reduce convergence time and generate detailed subsurface information. The developed method of seismic inversion based on HPSO has been tested with both synthetic and real data. In synthetic data, the inverted impedance trace closely follows the trend of real impedance, achieving correlation coefficients of 0.99. In real data, HPSO inversions exhibit high-resolution subsurface information, with impedance varying from 6000 to 16000 m/s∗g/cc and porosity from 1 to 30%. The interpretation of inverted sections identifies a low impedance (6000 to 9000 m/s∗g/cc) and high porosity (> 15%) anomaly in the time interval of 1040-1065 ms two-way travel time. This anomalous zone, also interpreted in well-log data, is characterized as a reservoir (sand channel).

ACKNOWLEDGMENTS

The authors would like to extend their appreciation to CGG Geo software for their generous provision of the Hampson Russell software and data, which significantly contributed to the success of this research. Furthermore, one of the authors, S.P. Maurya, expresses sincere gratitude to the funding agencies UGC-BSR (M-14-0585) and IoE BHU (Dev. Scheme no. 6031B) for their crucial financial support, which made this research possible. Special thanks are also owed to www.mathworks.com and www.norsar.no for providing academic licenses for Matlab (2022b). These invaluable resources played an essential role in the successful completion of this work.

Author Credit Statement

RK was involved in conceptualization, methodology design, software development and original draft writing. SPM supervised throughout the research. NV, RS and HR undertook thorough review and editing. APS, R, and KHS conducted validation. GH and PKK took charge of investigations. MKS conducted visualization.

Data availability

The authors do not have permission to share data..

Compliance with Ethical Standards

The authors assert the absence of any competing interests and adhere to copyright norms.

REFERENCES

Bonnans, J.F., Gilbert, J.C., Lemaréchal, C. and Sagastizábal, C.A., 2006. Numerical optimization: theoretical and practical aspects. Springer Science & Business Media.

Bosch, M., Mukerji, T. and Gonzalez, E.F., 2010. Seismic inversion for reservoir properties combining statistical rock physics and geostatistics: a review. Geophysics, 75(5),75A165-75A176

Broyden, C.G., 1970. The convergence of a class of double-rank minimization algorithms 1. General considerations. IMA J. Appl. Math., 6(1), 76-90.

Du, Z. and Macgregor, L.M., 2010. Reservoir characterization from joint inversion of marine CSEM and seismic AVA data using Genetic Algorithms: a case study based on the Luva gas field. In SEG Technical Program Expanded Abstracts. Society of Exploration Geophysicists, 737-741.

Dufour, J., Squires, J., Goodway, W.N., Edmunds, A. and Shook, I., 2002. Case History: Integrated geological and geophysical interpretation case study, and Lamé rock parameter extractions using AVO analysis on the Blackfoot 3C-3D seismic data, southern Alberta, Canada. Geophysics, 67(1), 27-37.

Hema, G., Maurya, S.P., Kant, R., Singh, A.P., Verma, N., Singh, R. and Singh, K.H., 2024. Enhancement of CO2 monitoring in the Sleipner field (North Sea) using seismic inversion based on simulated annealing of time-lapse seismic data. Marine Petrol. Geol., 106962.

Kant, R., Maurya, S.P., Singh, K.H., Nisar, K.S. and Tiwari, A.K., 2024a. Qualitative and quantitative reservoir characterization using seismic inversion based on particle swarm optimization and genetic algorithm: a comparative case study. Sci. Rep., 14(1),22581.

Kant, R., Kumar, B., Maurya, S.P., Singh, R. and Tiwari, A.K., 2024b. Exploring the utility of nonlinear hybrid optimization algorithms in seismic inversion: A comparative analysis. Phys. Chem. Earth, 103754.

Kumar, B., Kant, R. and Maurya, S.P., 2024. Qualitative and quantitative reservoir characterisation using seismic inversion based on global optimization: A comparative case study. J. Earth Syst. Sci., 133(2), 87.

Kushwaha, P.K., Singh, R., Maurya, S.P. and Rai, P., 2023. Prediction of petrophysical properties using post stack seismic inversion and geostatistical techniques over F-3 block, Netherlands-A comparative study. Int. J. Petrol. Technol., 10, 53-70.

Maurya, S.P. and Sarkar, P., 2016. Comparison of post-stack seismic inversion methods: a case study from Blackfoot Field, Canada. IJSER,7(8),1091–1101

Maurya, S.P. and Singh, N.P., 2018. Comparing pre-and post-stack seismic inversion methods-a case study from Scotian Shelf, Canada. J. Indian Geophys. Union, 22(6), 585-597.

Maurya, S.P. and Singh, N.P., 2020. Effect of Gaussian noise on seismic inversion methods. J. Indian Geophys. Union, 24(1), 7-26.

Maurya, S.P., Singh, N.P. and Singh, K.H., 2020. Seismic inversion methods: a practical approach. Springer.

Maurya, S.P., Singh, R., Mahadasu, P., Singh, U.P., Singh, K.H., Singh, R., Kumar, R. and Kushwaha, P.K., 2023. Qualitative and quantitative comparison of the genetic and hybrid genetic algorithm to estimate acoustic impedance from post-stack seismic data of Blackfoot field, Canada. Geophys. J. Int., 233(2), 932-949.

Nocedal, J. and Wright, S.J. eds., 1999. Numerical optimization. New York, NY: Springer New York.

Russell, B.H., Lines, L.R. and Hampson, D.P., 2003. Application of the radial basis function neural network to the prediction of log properties from seismic attributes. Expl. Geophys., 34, 15–23.

Shanno, D.F., 1970. Conditioning of quasi-Newton methods for function minimization. Mathematics of computation, 24(111), 647-656.

Simin, V., Harrison, M.P. and Lorentz, G.A., 1996. Processing the Blackfoot 3C-3D seismic survey. Crewes Res Rep, 8, 39- 1.

Singh, A.P., Maurya, S.P., Kant, R., Singh, K.H., Singh, R., Srivastava, M.K., Hema, G. and Verma, N., 2024. Implementing 4D seismic inversion based on Linear Programming techniques for CO2 monitoring at the Sleipner field CCS site in the North Sea, Norway. Acta Geophysica,1-23.

Received on: 30-09-2024 ; Revised on: 15-10-2024 ; Accepted on:18-11-2024